Title
A Dynamic 3D Culture System for Enucleation of MSCs to Reduce Lung Trapping

Permalink
https://escholarship.org/uc/item/5z66r78f

Author
Pi, Willie Mingyuen

Publication Date
2021

Peer reviewed|Thesis/dissertation

UNIVERSITY OF CALIFORNIA SAN DIEGO

A Dynamic 3D Culture System for Enucleation of MSCs to reduce Lung Trapping

A Thesis submitted in partial satisfaction of the requirement for the degree

Master of Science

in

Biology

by

Willie Mingyuen Pi

Committee in charge:

    Professor Richard Klemke, Chair
    Professor David Traver, Co-Chair
    Professor Gen-Sheng Feng

2021

The thesis of Willie Mingyuen Pi is approved, and it is acceptable in quality and form for publication on microfilm and electronically.

University of California San Diego

2021

Table of Contents

Table of Figures

ABSTRACT OF THE THESIS

A Dynamic 3D Culture System for Enucleation of MSCs to Reduce Lung Trapping

by

Willie Mingyuen Pi

Master of Science in Biology

University of California San Diego, 2021

Professor Richard Klemke, Chair
Professor David Traver, Co-Chair

Many mesenchymal stem cell (MSC) based therapies have the common issue of cells becoming trapped in the lung vasculature. Our novel enucleated cell therapy, named "Cargocytes," also encounter this issue, though to a lesser degree due to their smaller size. Lung trapping can be especially dangerous in a therapeutic because it can cause embolisms in the lung vasculature. We therefore designed and optimized a series of protocols to further reduce the cell size of these Cargocytes and obtain minimal lung trapping after intravenous injection. By using a spinner flask for 3D culture, we show

that the size of the MSCs and Cargocytes can be significantly reduced after 48 hours of culturing, as compared to cells cultured in a 2D environment. After optimizing the spinner flask culture, we then proceeded to optimize the enucleation process for 3D cells such that we could get a sufficient yield at an acceptable efficiency. We next compared the cell surface markers of 2D MSCs and 3D MSCs. Markers for MSCs remained constant even after culturing in 3D for 48 hours.

Because Cargocytes are a novel platform technology, some diagnostic assays have yet to be conducted on these new cell carriers. We conducted a series of tests to look at markers of apoptosis, such as an Annexin V and multi-caspase assay. We found the profiles to be comparable to that of the parental MSCs. Finally, we engineered hTERT-MSCs with exogenous CDK4 to potentially allow cells to grow under 3D culture conditions. Although the CDK4 engineering did not promote growth of MSCs in 3D conditions, the cells were able to survive much longer. A cell cycle analysis also revealed that these newly engineered cells have slightly more cells in the G2 phase compared to parental hTERT-MSCs.

Introduction

Bio-inspired biomimetic drug delivery carriers are becoming increasingly popular due to the need to protect unstable cargo from degradation [1]. In this thesis, we used mesenchymal stem cells (MSCs) due to their many therapeutic advantages. MSCs are known to have anti-inflammatory effects both in vivo and in vitro and can be used to treat inflammatory disease [2]. In the body, MSCs will naturally home to damaged tissue and release paracrine factors that promote regeneration and healing [3]. This homing mechanism occurs in four major steps: tethering, activation, arrest, and migration [4]. First, the cells tether to the endothelial cells via selectins. Chemokines, primarily SDF-1, then bind to receptors such as CXCR4 on the cell and in turn activate the cells to express VLA-4, which binds to the endothelial cells via VCAM-1 [4]. CXCR4 is not highly expressed in MSCs, and overexpression of CXCR4 has been shown to improve the homing capacity of the cells [5]. The MSCs then begin migrating toward chemokine gradients produced by the inflammatory or damaged tissue [3,4]. Knowing that these steps are critical to homing in MSCs, we designed and engineered MSCs to overexpress CXCR4, CCR2, and PSGL-1 with fucosyltransferase 7(fut7) to increase the homing capacity of our MSCs. However, in many in vivo experiments the homing of MSCs is not very efficient and obtaining autologous MSCs from patients can be time consuming and expensive [6].

Other delivery vehicles such as nanoparticles have an increased safety profile compared to MSCs [7] but are lacking in homing efficiency [8]. Bacterial and viral based carriers both have safety concerns, and synthetic mimetics have the risk of being recognized by the immune system and being eliminated before being able to deliver

1

their cargo [9]. Eukaryotic cells such red blood cells, macrophages and MSCs have lower immunogenicity, but they are all more difficult to produce compared to other synthetic carriers; they also have undefined life spans and may continue to circulate throughout the body [9]. MSC-derived exosomes are also an emerging platform due their small size and ability to cross the blood-brain barrier, while also preserving many of the same beneficial properties of their parental MSC [10]. Exosomes, however, are not as stable compared to cells; after recovery from cryopreservation the contents of the exosome may sometimes leak, and the exosomes tend to aggregate together [11].

To make up for the deficiencies in traditional cell therapies and nanoparticle technologies, we designed a new cell-based delivery platform designated "Cargocyte," where we engineer immortalized human telomerase reverse transcriptase (hTERT) MSCs with desired traits and then remove the nucleus via density gradient centrifugation. Base on unpublished data, we find that Cargocytes behave similarly to their parental MSCs and can sometimes home even better to inflamed tissue, partially due to the decreased lung trapping. In addition, they have a defined life span of approximately 72 hours and will not have unwanted long-term engraftment. Another added benefit is that due to the lack of a nucleus, the Cargocyte will not synthesize new RNA while circulating in-vivo. As a result, we have created a cell-like carrier with a higher safety profile as well as improved homing.

Despite extensive engineering, many MSCs do not home to diseased tissue in vivo because they become trapped in the lung after intravenous (i.v.) injection. This is partially due to the large size of the injected cells, which become obstructed by the smaller capillaries in the lungs [12]. In previous studies microspheres were injected into

2

mice intravenously, and many spheres the approximate size of MSCs (around 15 μm) were trapped in the lung vasculature, while smaller microspheres were found to bypass trapping as their size decreased [13]. When MSCs are cultured on 2D plates, a collection of integrins such as β1, α5, and αVβ3 are upregulated, and which may also contribute to an increase in lung trapping [14]. Lung trapping significantly decreased when these integrins were blocked using functional antibodies, thus suggesting that excessive integrins could also be one mechanism for MSC lung trapping [15]. Oftentimes, up to 80% of the MSCs are found trapped in the lung after intravenous infusion [16], causing embolisms that can be fatal for the mice. Culturing the MSCs in spheroids can decrease the cell size and integrin expression and may help in reducing lung trapping [17].

Aside from culturing mammalian cells on flat culture dishes, there are various ways to culture cells in 3D systems. Microcarriers are commonly used to culture adherent cell lines where each small sphere provides a surface for the cell to adhere and attach onto [21]. This method can be costly due to the need for microcarriers, as well as having to process out the microcarriers from the culturing solution. For smaller scale experiments, a hanging drop approach can be used where droplets of cells are inverted on a tissue culture plate [17]. The benefit of the static hanging drop system is that it is relatively inexpensive, and the equipment required is readily available, while microfluidic 3D culture systems are useful for high-throughput screening and testing purposes [18]. For industrial level scale ups, stirred flasks are commonly used and can culture up to billions of cells [19].

3

In this thesis, we focus on the issue of MSCs becoming trapped in the lung after i.v. injection. To solve this problem, we combined enucleation and an optimized 3D culture system to build up a new delivery platform that has minimum lung trapping.

Results

Selecting for Small Size via FACS does not Result in Consistent Reduced Cell Size

We first investigated to see if there was a simple, straightforward way to sort out a population of smaller cells via FACS. In flow cytometry, forward scatter (FSC) measures the cell size; we selected for the top 1% of smallest cells using FSC and cultured them for 2 weeks. The FSC mean for the unsorted cells was 193,886 (Figure 1D) and after a week of growth the FSC mean for the sorted cells was 178,376 (Figure 1A). After 2 weeks we measured the sorted cells again and found that the FSC had increased to 190,076 (Figure 1B). We sorted the cells for a second time, and the FSC mean was higher than the cells that were sorted one time only (Figure 1C). The cells did not maintain their small size and continue to expand regardless of how many times we sorted them. This is likely due to the cells naturally growing larger in vitro as they were passaged closer to senescence [20]. We then decided to move on to using a 3D culturing method to decrease the cell size.

Dynamic Spinner Flask Culture Reduces Cell Size

Our previous experiments show that 3D culture using hanging drop results in a smaller MSC that can be readily enucleated. However, this process can be highly laborious and is not easily scalable. As a result, we decided to focus on spinner flask dynamic culture. We first cultured cells in the spinner flask and found that many cells began to stick and adhere to the sides of the glass vessel, forming large clumps that were unable to be dissociated using Accutase. We found that adding Sigmacote to the glass before autoclaving solved this problem. Based on previous studies [21] we found

that a speed of 30 rotations per minute (rpm) resulted in large clumps of cells that were unable to be easily dissociated with Accutase (Figure 3A), while higher speeds around 100 rpm resulted in many cells dying due to sheer stress. We eventually settled on 60 rpm for this specific spinner flask for a balance between ease of dissociation and cell viability. A culture time of 48 hours was also found to be an appropriate time to maximize cell viability and minimize cell size. Initially, after inputting approximately 4.0×10^7 cells into the spinner flask, less than 50% of the cells were recovered from the flask after processing and filtering (Figure 2B). After incubating the cells on ice for 1 hour prior to placing them in the spinner flask, we greatly increased the yield of cells from the spinner flask. This critical incubation step was preserved in later versions of our protocol. For the rest of the experiments involving the spinner flask, we consistently got above 60% yield for 3D cells that were incubated on ice (Figure 2B, n=6). Throughout the various runs, the cell size was also reduced significantly (Figure 2C) after undergoing 3D culture for 48 hours.

3D Cells can be Enucleated

To optimize for enucleation efficiency, we started by using our previously established protocol for enucleation 2D cells. Through our initial runs, we found the 2D enucleation protocol to be insufficient and often resulted in a low yield and efficiency (Figure 3B). In our original protocol for enucleating 2D cells, 20 million cells was the upper limit we would input into the tube for centrifugation. We experimented with a longer centrifugation time by extending the spin time to 75 minutes (Figure 3D). This resulted in a lower efficiency compared to the control protocol (Figure 3C). Next we decided to load 40 million cells into the tube and also add 2 times the amount of

6

Cytochalasin B to the solution (this weakens the cytoskeleton which allows to nucleus to more easily break free). This resulted in a greatly improved yield and we were able to consistently get greater than 40% yield from each run, as well as approximately 70-80% efficiency of enucleation (Figure 3E). Another critical step was also to input the cells into the spinner flask when the plates were at a density of around 3.5 million per 15 cm plate. Each run loaded with 40 million cells yielded at least 15 million Cargocytes, which were then processed for further animal experiments.

3D Culturing Reduces Lung Trapping in Vivo

After optimizing the spinner flask and enucleation process, we then proceeded to test our hypothesis in-vivo by injecting mice with Vybrant-DiD (DiD) labelled Cargocytes and MSCs intravenously. As seen in previous experiments, the lung trapping was reduced from 2D cells to Cargocytes due to their reduced size (Figure 2E). We see that the lung trapping is greatly decreased when comparing Cargocytes to MSCs, most likely due to the removal of the nucleus and the increased deformability of the cell. In addition, 3D culturing further decreases lung trapping when comparing the 3D MSCs and Cargocytes to their 2D counterparts.

3D cells Share Similar Markers Compared to 2D Cells

Our previous profiling work done on 2D MSCs and Cargocytes showed that MSC markers were unchanged after enucleation. We then decided to assess whether the 3D culturing of MSCs were changing the MSCs to some other cell type. To assess the cell surface markers of 3D cultured cells, we used flow cytometry to look for the presence of CD44, CD90, CD105, and CD166, as well a lack of CD45. Cells are categorized as MSCs when they are positive for CD44, CD90, CD105, and CD166 while lacking

7

hematopoietic markers such as CD45 [23]. We found that the 3D cultured cells shared a cell surface marker profile comparable to 2D cells, with the exception of CD45, where there was a weak signal (Figure 4C).

In addition, 3D-cultured MSCs that are enucleated are also able to be transfected with exogenous mRNA and translate protein in-vivo. Mice were injected with LPS in the right ear intradermally (i.d) and then injected with human IL-10 transfected MSCs or Cargocytes (Figure 4F). ELISA results show that not only can 3D cells be enucleated, but they can also be transfected with mRNA, produce the desired protein, and deliver it to the site of injury. 3D Cargocytes are also able to spread and attach to tissue culture plates that have been coated with fibronectin (Figure 4E).

Cargocytes Die in a Similar Manner Compared to MSCs

Because Cargocytes do not have nuclei, they have a defined lifespan and will undergo cell death. We hypothesize that some Cargocytes may die via apoptosis and conducted a series of tests to look for phosphatidylserine and caspase activity. Using Actinomycin D as the positive control for the multi-caspase assay, we found that an increase in caspase activity is seen 24 hours after Cargocytes are plated onto tissue culture dishes (Figure 4A). For Annexin V staining, we heat shocked the cells at 45ºC as the positive control for apoptosis. Similarly, we saw a steady decrease in the apoptotic population with each increasing time point, with the biggest change occurring from the 48 to 72-hour time point. These two assays suggest that a portion of the Cargocytes may be undergoing apoptotic cell death mechanisms. However, more assays need to be done to check for other forms of cell death, such as immunogenic cell death. We also conducted a sodium dodecyl sulphate polyacrylamide gel electrophoresis (SDS-

PAGE) on 2D Cargocytes at different time points (Figure 4D). The protein bands are consistent at each time point. The faint band at the bottom of the MSC control lane can most likely be attributed to histones.

hTERT MSCs can be Engineered to Express Exogenous CDK4

Although the hTERT-MSCs are cultured in 3D spinner flask vessels, the cells do not proliferate, and instead decrease over time. CDK4 has been shown to help cells overcome cellular senescence [24]. As a result, we decided to engineer hTERT MSCs with exogenous CDK4 expression using a lentiviral vector. The vector contains an EGFP reporter (Figure 5A), and we confirmed the expression of the CDK4 via immunostaining using an PE conjugated anti-CDK4 antibody. We then decided to look at the cell cycle profile of the newly engineered hTERT-CDK4 cells. We saw a slight increase in the G2 population for the hTERT-CDK4 cells: the 2D hTERT MSCs had 8.49% of the population in the G2 phase and the 2D hTERT-CDK4 MSCs had 10.3% of the population (Figure 5B). Additionally, we also analyzed hTERT-CDK4 cells that were in 3D culture conditions and found only 3.91% of the population were in G2 phase. This suggests that the cells are not growing under 3D conditions. Curiously, the CDK4 cells were placed under the same 3D culture conditions as described in our protocol, and many cells were viable even up until 10 days and 19 days (Figure 5D). Although we did not see any cell growth in these cultures, we observed a mixture of spheroid structures as well as single cells. With un-engineered hTERT-MSCs most of the cells were dead or clumped by the later days and could not be accurately counted. This data could potentially be useful for the development of an MSC cell culture that can be cultured in a

9

single cell suspension, which would be valuable for scaling up Cargocytes for industrial
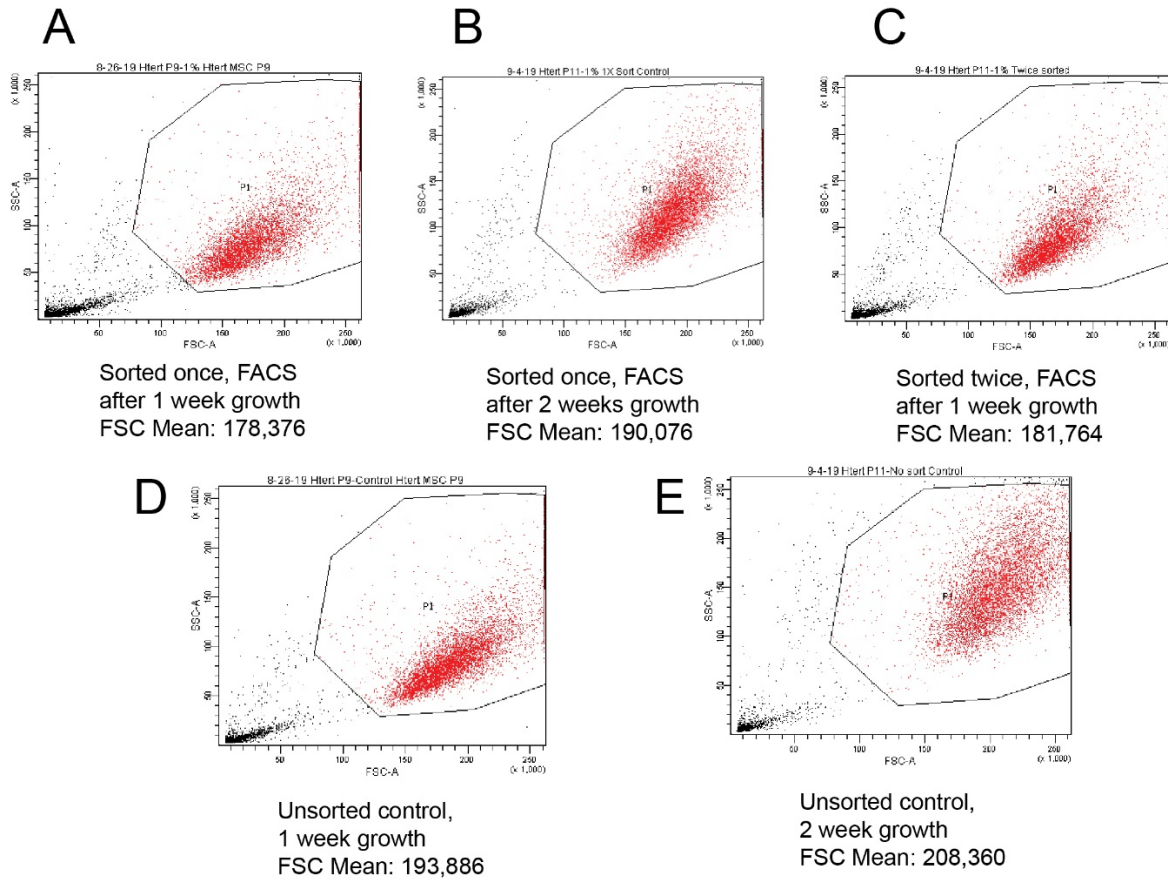
manufacturing.

Figure 1. Selecting for size via flow cytometry does not educe cell size. (A) hTERT MSCs sorted and measured of 1 week of growth. (B) sorted hTERT MSCs measured after 2 weeks of growth. (C) Cells from (B) were sorted again and measured after another week of growth. (D) and (E) are control cells at 1 week and 2 weeks without any sorting.
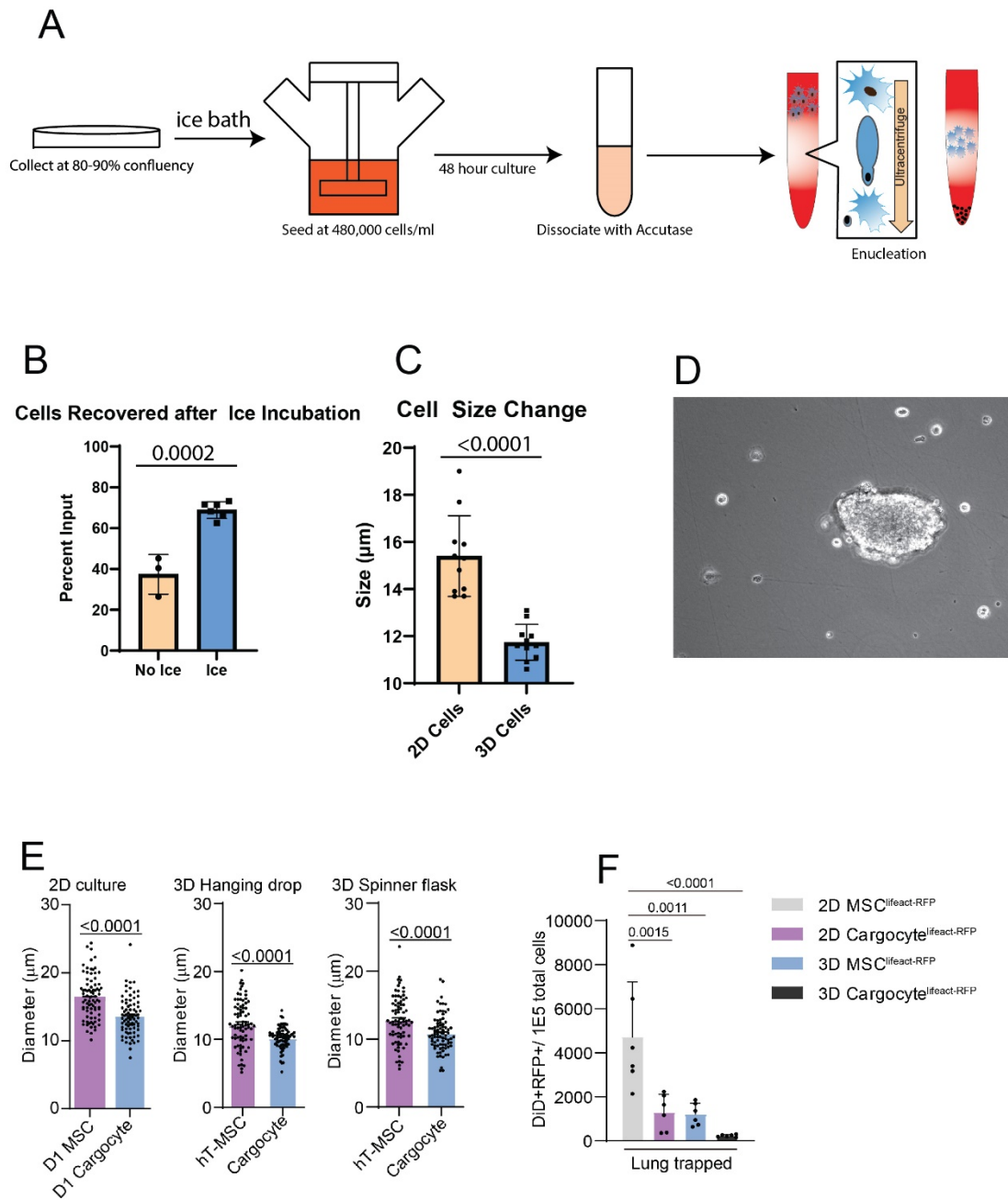
Figure 2. MSCs cultured in spinner flasks show significantly reduced size and reduced lung trapping. (A) Schematic of workflow for optimal 3D culture and enucleation. (B) Cells that were incubated in ice prior to seeding into spinner flask had a significantly increased survival rate. (C) MSC cell size changed significantly after culturing for 48 hours in a spinner flask. (D) Brightfield image of typical clumped cells found in spinner flask that are unable to be dissociated via Accutase. (E) Size comparison between cells and Cargocytes in each culture method. (F) MSCs labeled with Vybrant DiD injected into lungs were counted using a FACSCanto II cytometer. Trapping significantly decreased between the 2D and 3D MSCs.
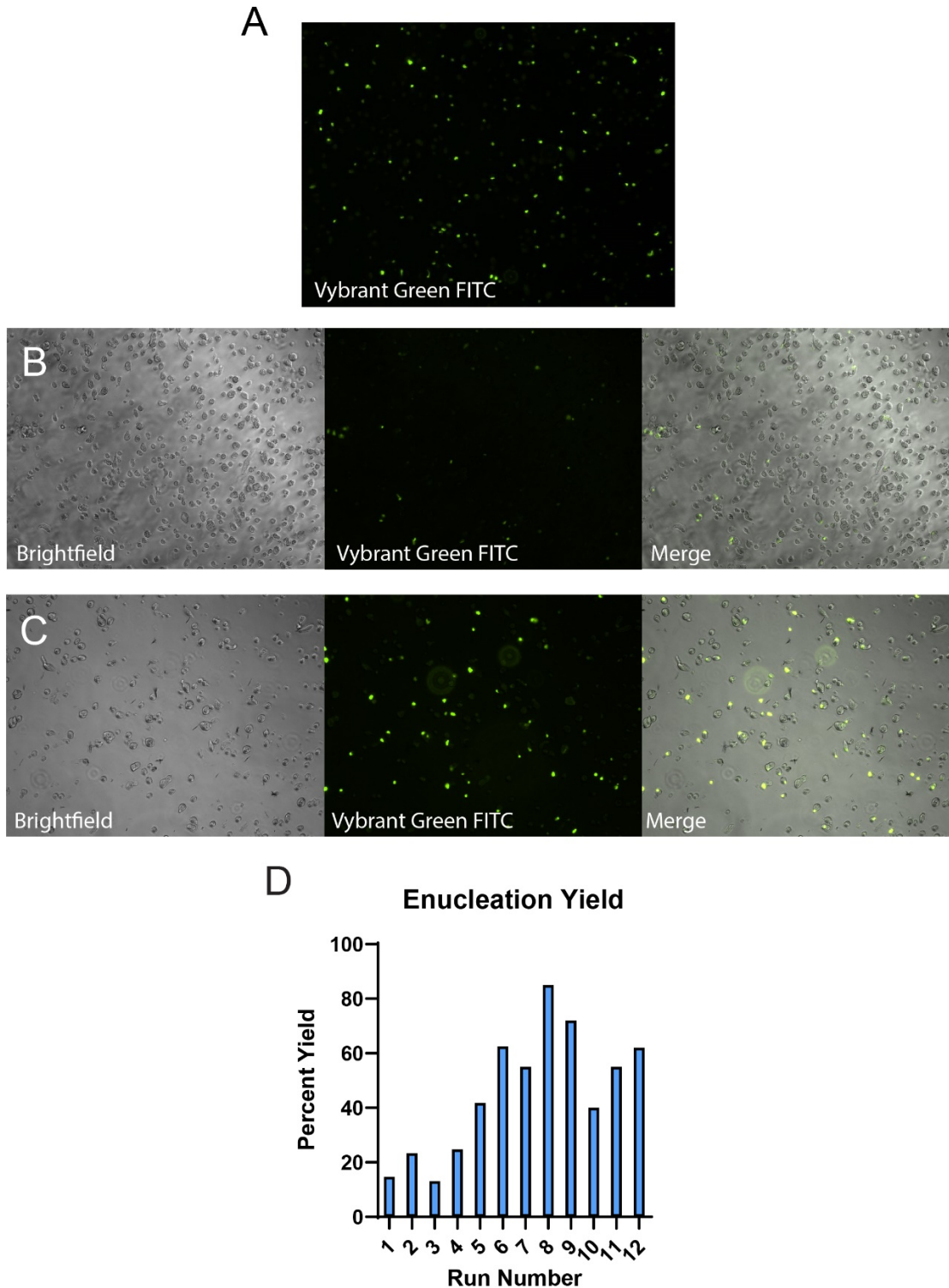
Figure 3. 3D MSCs can be enucleated. (A) Early enucleation runs showing low efficiency for 3D enucleation. Vybrant Green dye was used to label the nuclei. (B) Efficient 3D enucleation showing low number of nuclei present. (C) Results of experimenting with a longer enucleation time. Cells were spun in the centrifuge for an additional 15 minutes, which resulted in a lower enucleation efficiency. (D) Enucleation yield optimized to yield around 40% of the input in later runs. All runs after run 6 used twice the amount of Cytochalasin and 40 million cells as the minimum load amount.
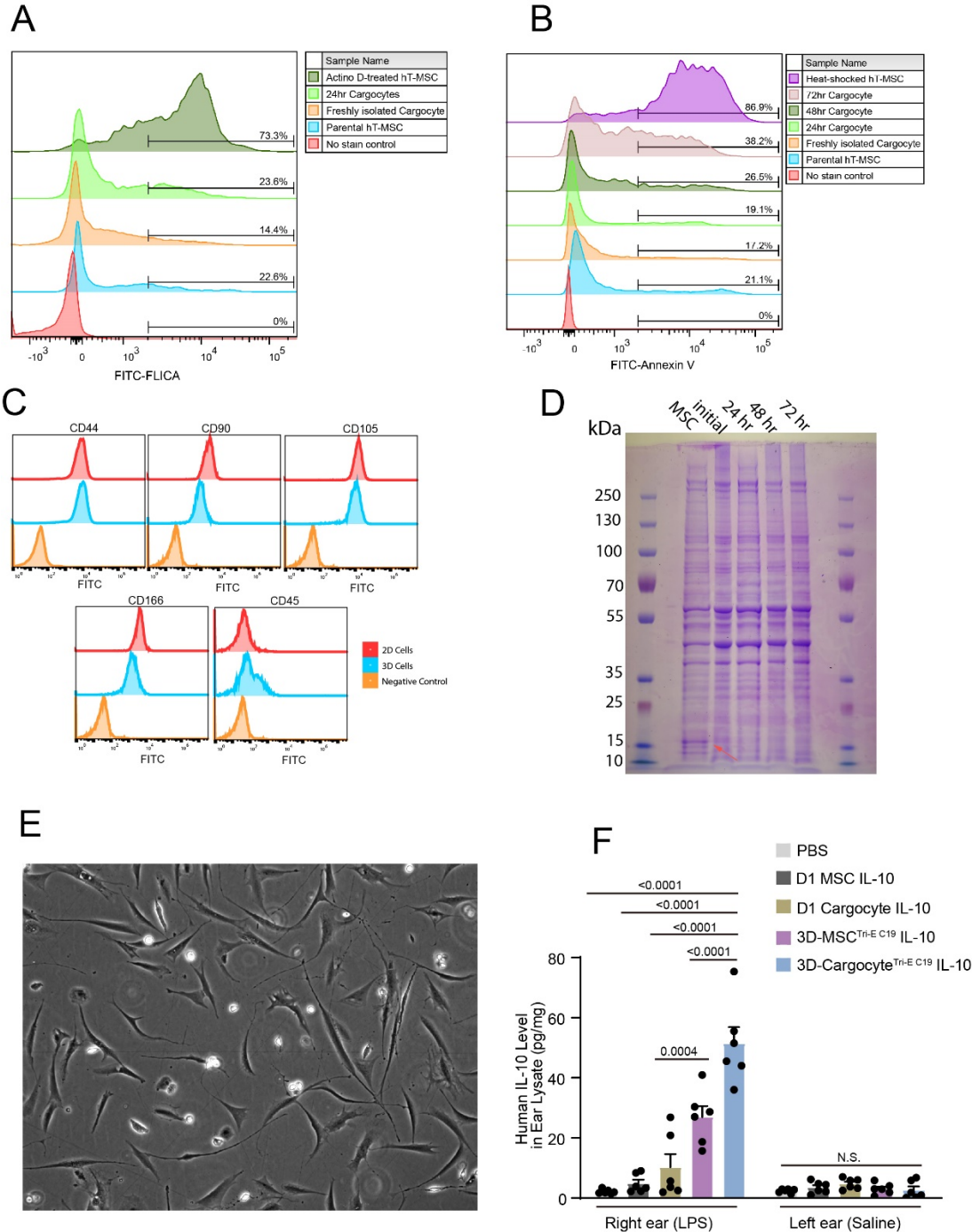
Figure 4. Cargocytes and MSCs undergo similar death mechanisms; 3D Cargocytes are functionally comparable to 2D Cargocytes. (A) A multi-caspase assay analysis of 2D Cargocytes after 24 hours of plating onto culture dishes. Actinomycin D was used as the positive control for caspase activity. (B) Annexin V analysis of 2D Cargocytes at different time points via flow cytometer. Heat shock was used for positive Annexin V control. (C) MSC marker panel comparing 2D cells and 3D cells cultured in spinner flasks for 48 hours. (D) Commassie blue stained SDS-PAGE showing bands for Cargocytes at different time points after plating. Red arrow points to potential histone location in the MSC control. (E) Brightfield image of 3D Cargocytes plated onto Fibronectin coated plates and spreading. Image was taken 24 hours after 3D cells were enucleated and plated. (F) ELISA analysis showing ability of 3D Cargocytes to translate human IL-10 mRNA and deliver it to an inflamed ear.

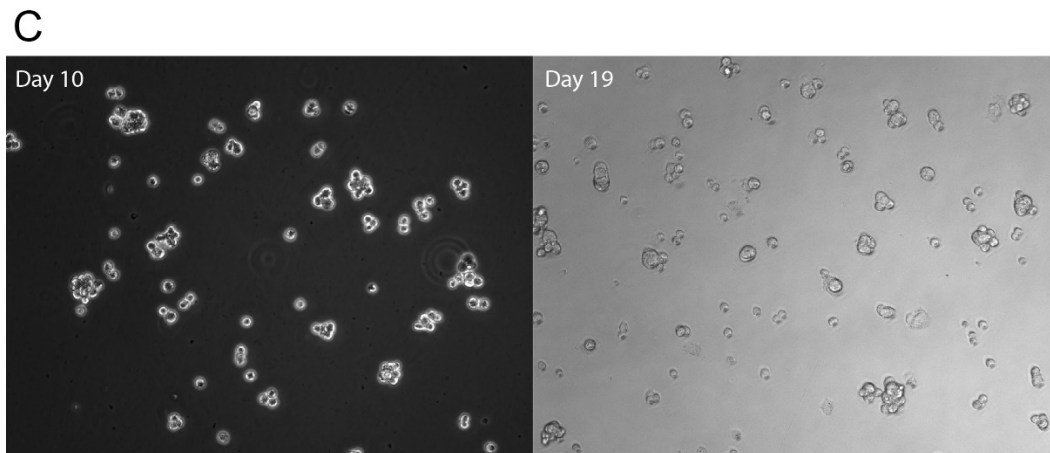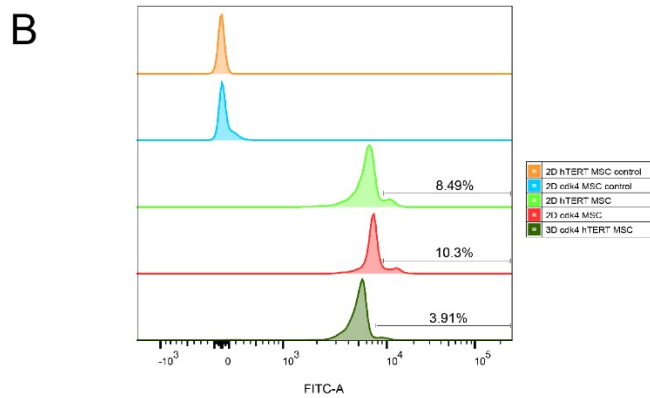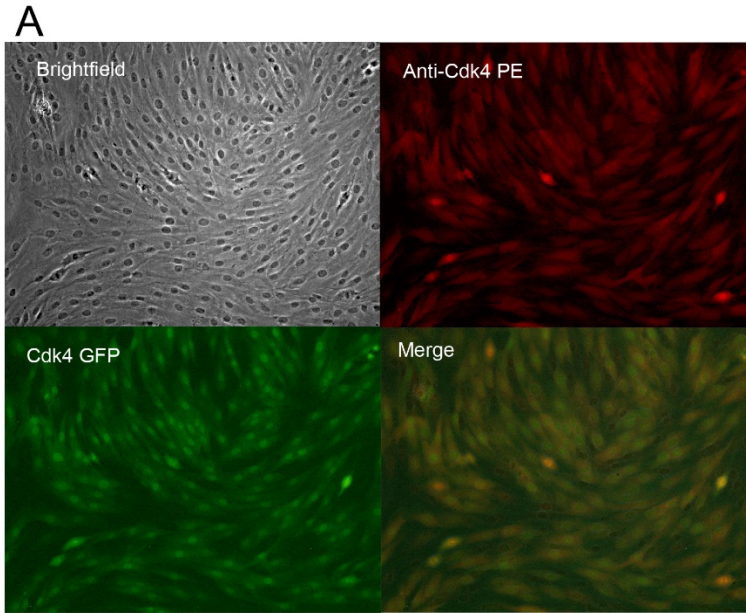**Figure 5. hTERT-MSCs can be engineered to express exogenous CDK4.** (A) hTERT-CDK4 MSCs stained with PE anti-CDK4 antibody. The lentiviral vector contains a GFP reporter gene. (B) Cell cycle analysis was done using Vybrant Green dye for 2D CDK4 MSCs, 2D hTERT MSCs, and 3D CDK4 MSCs. Indicated percentages represent population of cells in the G2 phase. (C) CDK4 MSCs under spinner culture conditions at indicated time points.

Discussion

In this thesis, we describe how the combination of enucleation and 3D spheroid culture greatly decreases the number of MSCs trapped in the lung vasculature. Our initial effort to select for a population of smaller cells via flow cytometry sorting was unsuccessful: the cells would expand in size over time despite sorting and selecting for the top 1% smallest cells. MSCs and stem cells in general tend to undergo senescence and expand in size as the passage number increases [20]. It is likely that the small selected cells did not have any significant genetic differences from larger cells that contributed to the size difference. We then decided to use spheroid formation via spinner flasks as the primary form of shrinking down cell volume. Spheroid formation occurs in three steps: aggregation, delay, and compaction [25]. Initially, the cadherins and integrins interact with each other and loosely associate together. During the delay period the cells reorganize and begin to start the compaction process [25]. In other published protocols, we find that that the compaction process has extended too far [26] and thus dissociation became difficult. The parameters we set along with the 48-hour time point seemed to be optimal for our needs, especially considering that the cells were required to undergo a stressful enucleation process afterwards. Through optimizing the culture time, spinner flask impeller speed, and density, we have achieved a consistent yield of greater than 60% 3D cells. Spheroid MSCs also have increased anti-inflammatory properties compared to 2D cultured MSCs [17], and when co-cultured with macrophages spheroid MSCs also decrease secretion of TNF-α. Previously published protocols often use stronger dissociation reagents such as trypsin [22], but

15

we found that the trypsin was too harsh on the cell surface receptors we engineered onto the MSC's surface.

After enucleation, we found that fewer 3D Cargocytes are trapped in the lungs compared to the parental 3D MSCs. We believe that this is due to the combination of 3D culturing and enucleation: enucleation removes the rigid nuclei and makes the cell more deformable, while 3D culturing further reduces the size and potentially changes the integrin profile. Certain integrins become downregulated in 3D culture and are thought to be significant in reducing lung trapping [14]. In previous studies, we found that Cargocytes maintain most of their cell membrane proteins and receptors. Therefore, we can infer that if the integrin profile of the 3D Cargocytes and 3D MSCs are similar, size also plays a significant role in reducing lung trapping. A more thorough study of the integrins being upregulated and downregulated for 2D and 3D culture would give us more insight for reducing lung trapping, such as re-engineering the MSCs with different integrins.

In addition to optimizing 3D enucleation of Cargocytes, we also looked at potential ways in which Cargocytes die. Due to the lack of a nucleus, Cargocytes undergo cell death within 96 hours. After conducting Annexin V and multi-caspase assays, we found that the profile of Cargocytes and the parental MSCs are mostly similar. Apoptosis biomarkers include detection of series of caspases activating a signal cascade to amplify death signals, as well as the exposure of phosphatidylserine to the outer plasma membrane [27], which is detected by Annexin V staining. One major concern for cell-like delivery platforms is the potential of immunogenic cell death, where the cells are attacked before successfully delivering the cargo. The current gold

16

standard for detecting immunogenic cell death is detection of calreticulin on the surface and extracellular ATP and high mobility group box protein 1 (HMGB1) [28]. Eliminating immunogenic cell death as the death pathway for Cargocytes would require these assays to be conducted.

Finally, we generated a hTERT-CDK4 MSC (CDK4 MSC) for the purpose of studying single cell suspension cell growth. Given that we observed no growth in hTERT-MSCs being cultured in 3D culture flasks, we hypothesized that engineering in CDK4 could potentially help the cells overcome senescence [25]. As observed in our cell cycle analysis, there is a slight increase in cells in the G2/M phase in CDK4 MSCs compared to parental hTERT MSCs. However, cells in the G2/M phase are still greatly decreased in 3D cultured CDK4 cells, suggesting that CDK4 is not sufficient for initiating growth for traditionally adherent cells in suspension culture. In the past, the simian vacuolating virus 40 (SV40) antigen has been used to transform adherent cells into anchorage independent cells [29]. The disadvantage of these more drastic engineering solutions is that it could transform the MSC into a different cell that is no longer useful for therapeutic purposes.

Here, we provide the basis for an improved MSC delivery vehicle that has greatly reduced lung trapping and potential for industrial scale up. Enucleation or 3D culturing alone will both reduce the number of cells trapped in the lung vasculature (Figure 2F) but combining the two together produces a synergistic effect which drastically decreases lung trapping when compared to 2D MSCs. These 3D Cargocytes are more deformable, smaller, and able to home better than traditional MSCs cultured on flat tissue culture dishes while still maintaining many of the critical characteristics and

markers that are essential for a successful cargo delivering therapeutic. However, more research and optimization need to be conducted to elevate enucleation efficiencies to higher percentages. Developing a method to grow MSCs in anchorage-independent suspension cultures could be incredibly powerful for large scale manufacturing purposes. A finalized Cargocyte product would be able to carry many different types of cargo, easy to manufacture to scale, as well as having highly effective homing potential with reduced lung trapping.

Cell Culture

Immortalized human telomerase reverse transcriptase adipose-derived MSCs (hTERT-MSCs) were purchased from ATCC (#SCRC-4000). MSCs were cultured in alpha MEM (Gibco #12561) supplemented with 16.5% Premium FBS (Atlanta Biologics S1150), 1% HEPES (Gibco #15630), 1% Glutamax 100X (Gibco #35050), and 1% Anti-Anti 100X (Gibco #15240). 293T cells were cultured in DMEM (Gibco #11960) with 10% FBS.

Flow Cytometry

MSCs or Cargocytes were stained with 10 µM Vybrant DiD (Invitrogen, #V22887) following manufacturer's instructions prior to injection. MSCs or Cargocytes were washed in FACS buffer (pH 7.4 PBS, 1% FBS) and stained with antibodies for 30 minutes on ice. After washing with FACS buffer 2 times, samples were analyzed by the FACS Canto II (BD). For Annexin V staining, cells were stained according to manufacturer's instructions using the cell death assay kit (Biolegend, #640922). The Vybrant FAM Poly Caspases assay kit (Thermo Fisher, #V35117) was used for the caspase assay. Cell sorting was done at the UCSD Stem Cell Core using an FACSAria Fusion sorter (BD).

Animal Experiments

All animal experiments were executed according to ACP guidelines listed in our animal protocol #S12500. Briefly, mice were injected with a lipopolysaccharide (LPS) intradermally in the right ear and with saline in the left ear. MSCs or Cargocytes were injected 6 hours post LPS injection, and lungs and ears were harvested at the appropriate time points. For tissue processing, lungs were digested using collagenase

and filtered through 70 µm strainers, lysed with red blood cell lysis buffer (Biolegend, #420301) and stained with PE anti-mouse F4/80 antibody and 7-AAD. Cells were analyzed using a FACS Canto II.

ELISA

Ears were homogenized in lysis buffer using the AG Polytron PT1200. Lysis buffer contains PMSF (Thermo Scientific, #36978) and a cocktail of protease inhibitors (Roche, #11697498001). Lysates were diluted and loaded onto ELISA kits (Biolegend, #430604) according to manufacturer instructions. Absorbance was read using the µQuant plate reader (Biotek).

Hanging Drop Culture

Briefly, cells were resuspended in 35 µl of medium at 30,000 cells per drop. Drops were plated on the lid of a tissue culture plate and inverted. 5 mls of PBS was added in the plate to prevent evaporation of droplets. After approximately 40 hours, cells were harvested and dissociated using Accutase (Innovative Cell Technologies, #AT104-500) and 100 µg/ml DNAse I (Sigma Aldrich, #10104159001). Cells were finally passed through a 70 µm strainer (BioPioneer, #DGN258368).

Spinner Flask culture

Briefly, spinner flasks (Corning, #4500-500) were coated with 2-3 mls of Sigmacote (Sigma, SL2-100ML) to prevent excess cell adhesion. Flasks were recoated with Sigmacote every 2 runs to prevent cells from further adhering. MSCs were grown to 3-4 million cells per 15 cm tissue culture plate (Olympus Plastics, #25-203) and seeded at a density of 4.8×10^5 cells per ml in the spinner flask (Corning, #4500-500). On the day of collection, 50 million cells were collected using Accutase and incubated on ice for 1

hour before adding into the spinner flask. Cells were cultured at 37 °C for 2 days with 5% CO_2 at 60 rpm. At 24 hours, medium was added to the flask to get a final concentration of 4.0×10^5 cells per ml. To obtain a single cell suspension, cells were collected from the spinner flask after 2 days and incubated with Accutase for 15 minutes in a 37°C water bath. Cells were pipetted every 5 minutes to promote dissociation, then passed through a 70 µm cell strainer to obtain a single cell suspension.

Enucleation

For enucleation, Ficoll PM400 (GE Healthcare, #17-0300-500) was dissolved into a 50% wt/wt solution with ultrapure water (Invitrogen, #10977-015), autoclaved, aliquoted, and stored at -20°C. Ficoll gradients were made with 50% Ficoll and 2X MEM (Gibco, #11430) to create 25%, 17%, 16%, 15%, and 12.5% solutions. Cytochalasin B (Sigma Aldrich, #C6762) was added while making the 2X MEM to a final concentration of 20 µg/ml. Ficoll solutions were layered into 13.2 ml centrifuge tubes (Beckman Coulter, #344059) at decreasing density using a syringe and equilibrated overnight at 37°C in a tissue culture incubator. The following day, cells were harvested from the spinner flasks and resuspended in 3.2 ml of 12.5% Ficoll. 1 ml of 1X MEM was added to the top layer. An SW41 rotor was used and tubes were run in a Beckman Coulter L8-60M centrifuge for 60 minutes at 31°C. Cells were washed using serum-free medium and then a sample was stained with Vybrant DyeCycle Green (Invitrogen, #V35004). To observe efficiency a Nikon Eclipse TI epifluorescence microscope was used with the NIS-Elements AR 3.0 software (Nikon).

MSC Marker Panel

An antibody kit was used for all staining (R&D Systems, #SC017). Around 1.0x10^6 MSCs were collected and washed with PBS once. Cells were resuspended in 90 ul FACS buffer (1% FBS in PBS) and 10 ul of each primary antibody was added (CD44, CD90, CD105, CD166, CD45). After a 30-minute incubation period at room temperature, cells were washed twice with 2 ml FACS buffer and resuspended in 200 ul buffer and 1 ul secondary antibody. After a 30-minute room temperature incubation, cells were washed twice as in previous steps and analyzed using the flow cytometer.

CDK4 Transduction

pHAGE-CDK4 was a gift from Gordon Mills and Kenneth Scott (Addgene plasmid #116724; http://n2t.net/addgene:116724; RRID: Addgene_116724) [30]. Briefly, lentivirus was generated using a second-generation packaging system and 293T cells. hTERT MSCs were transduced with lentivirus particles in Opti-MEM medium (ThermoFisher, #31985088) with 8 µg/ml SureENTRY transduction reagent (Qiagen, #336921). To check for successful transduction, cells were viewed under an epifluorescence microscope for EGFP.

Immunofluorescence Staining

CDK4 MSCs were plated at around 1M per 6 well plate. Cells were fixed using 4% PFA for 15 min at room temperature, then permeabilized with 0.2% Triton X-100 in PBS with 5% normal goat serum for 10 minutes at room temperature. Anti-cdk4 antibody (Santa Cruz Biotechnology, sc-23896) was diluted 1:500 and 200 ul of the antibody solution was added to each well. Cells were incubated overnight and washed gently with PBS the next day 3 times. Cells were observed using the Nikon epifluorescence microscope.

SDS-PAGE

hTERT Cargocytes were plated on Fibronectin coated plates and collected at 24, 48, and 72 hours post enucleation. Cells and Cargocytes were flash frozen in liquid nitrogen and stored in -80C before use. Samples were processed using RIPA buffer. After obtaining the concentration of the samples using a BCA assay (ThermoFisher, #23225), each lane on the nuPAGE gel (Thermo Fisher, NP0323BOX) was loaded with 10 ug of protein. The gel was run at 135V for 90 min, washed in de-ionized (DI) water briefly, and stained using G250 for 5 min. After staining the gel was washed briefly using 10% acetic acid, 40% methanol solution in DI water until faint bands were seen. The gel was then soaked in DI water overnight to visualize clear bands.

Cell Cycle Analysis

Cells were harvested using Accutase and resuspended in 1 ml full serum medium. 2 µl of Vybrant® DyeCycle™ Green Stain (5 mM) was added and cells were incubated at 37°C for 30 min protected from light and analyzed using the flow cytometer.

Statistical Analysis

All statistical analysis was conducted on GraphPad Prism 9 using unpaired Student's t-test and one-way ANOVA.

References

1. Young, J. S., Kim, J. W., Ahmed, A. U., & Lesniak, M. S. (2014). Therapeutic cell carriers: a potential road to cure glioma. *Expert review of neurotherapeutics*, *14*(6), 651–660. https://doi.org/10.1586/14737175.2014.917964

2. Gao, F., Chiu, S. M., Motan, D. a. L., Zhang, Z., Chen, L., Ji, H.-L., Tse, H.-F., Fu, Q.-L., & Lian, Q. (2016). Mesenchymal stem cells and immunomodulation: Current status and future prospects. *Cell Death & Disease, 7*(1), e2062–e2062. https://doi.org/10.1038/cddis.2015.327

3. Ullah M, Liu DD, Thakor AS. Mesenchymal Stromal Cell Homing: Mechanisms and Strategies for Improvement. *iScience*. 2019;15:421-438. doi:10.1016/j.isci.2019.05.004

4. De Becker A, Riet IV. Homing and migration of mesenchymal stromal cells: How to improve the efficacy of cell therapy?. *World J Stem Cells*. 2016;8(3):73-87. doi:10.4252/wjsc.v8.i3.73

5. Yang JX, Zhang N, Wang HW, Gao P, Yang QP, Wen QP. CXCR4 receptor overexpression in mesenchymal stem cells facilitates treatment of acute lung injury in rats. *J Biol Chem*. 2015;290(4):1994-2006. doi:10.1074/jbc.M114.605063

6. Regmi, S., Pathak, S., Kim, J. O., Yong, C. S., & Jeong, J.-H. (2019). Mesenchymal stem cell therapy for the treatment of inflammatory diseases: challenges, opportunities, and future perspectives. *European Journal of Cell Biology.* doi:10.1016/j.ejcb.2019.04.002

7. Fang RH, Kroll AV, Gao W, Zhang L. Cell Membrane Coating Nanotechnology. *Adv Mater*. 2018;30(23):e1706759. doi:10.1002/adma.201706759

8. Lutz H, Hu S, Dinh P-U, Cheng K. Cells and cell derivatives as drug carriers for targeted delivery. *Medicine in Drug Discovery*. 2019;3:100014. doi:https://doi.org/10. 1016/j.medidd.2020.100014

9. Yoo JW, Irvine DJ, Discher DE, Mitragotri S. Bio-inspired, bioengineered and biomimetic drug delivery carriers. *Nat Rev Drug Discov*. 2011;10(7):521-535. Published 2011 Jul 1. doi:10.1038/nrd3499

10. Yin, K., Wang, S. & Zhao, R.C. Exosomes from mesenchymal stem/stromal cells: a new therapeutic paradigm. *Biomark Res* 7**,** 8 (2019). https://doi.org/10.1186/s40364-019-0159-x

11. Baharlooi H, Azimi M, Salehi Z, Izad M. Mesenchymal Stem Cell-Derived Exosomes: A Promising Therapeutic Ace Card to Address Autoimmune Diseases. *Int J Stem Cells*. 2020;13(1):13-23. doi:10.15283/ijsc19108

12. Fischer UM, Harting MT, Jimenez F, Monzon-Posadas WO, Xue H, Savitz SI, Laine GA, Cox CS Jr. Pulmonary passage is a major obstacle for intravenous stem cell delivery: the pulmonary first-pass effect. *Stem Cells Dev.* 2009 Jun;18(5):683-92. doi: 10.1089/scd.2008.0253.

13. Schrepfer, S., Deuse, T., Reichenspurner, H., Fischbein, M. P., Robbins, R. C., & Pelletier, M. P. (2007). *Stem Cell Transplantation: The Lung Barrier. Transplantation Proceedings, 39(2), 573–576.* doi:10.1016/j.transproceed.2006.12.019

14. Wang, S., Guo, L., Ge, J., Yu, L., Cai, T., Tian, R., Jiang, Y., Zhao, R. C., & Wu, Y. (2015). Excess Integrins Cause Lung Entrapment of Mesenchymal Stem Cells. *STEM CELLS*, *33*(11), 3315–3326. https://doi.org/10.1002/stem.2087

15. Zhou Y, Chen H, Li H, Wu Y. 3D culture increases pluripotent gene expression in mesenchymal stem cells through relaxation of cytoskeleton tension. *J Cell Mol Med*. 2017;21(6):1073-1084. doi:10.1111/jcmm.12946

16. Lee, R. H., Pulin, A. A., Seo, M. J., Kota, D. J., Ylostalo, J., Larson, B. L., Semprun-Prieto, L., Delafontaine, P., & Prockop, D. J. (2009). Intravenous hMSCs improve myocardial infarction in mice because cells embolized in lung are activated to secrete the anti-inflammatory protein TSG-6. *Cell stem cell*, *5*(1), 54–63. https://doi.org/10.1016/j.stem.2009.05.003

17. Bartosh, T. J., Ylöstalo, J. H., Mohammadipoor, A., Bazhanov, N., Coble, K., Claypool, K., Lee, R. H., Choi, H., & Prockop, D. J. (2010). Aggregation of human mesenchymal stromal cells (MSCs) into 3D spheroids enhances their antiinflammatory properties. *Proceedings of the National Academy of Sciences of the United States of America*, *107*(31), 13724–13729. https://doi.org/10.1073/pnas.1008117107

18. Breslin S, O'Driscoll L. Three-dimensional cell culture: the missing link in drug discovery. *Drug Discovery Today*. 2013;18(5):240-249. doi:10.1016/j.drudis.2012.10.003

19. Petry F, Weidner T, Czermak P, Salzig D. Three-Dimensional Bioreactor Technologies for the Cocultivation of Human Mesenchymal Stem/Stromal Cells and Beta Cells. Papantoniou I, ed. *Stem Cells International*. 2018;2018:2547098. doi:10.1155/2018/2547098

20. Yang, Y.-H. K., Ogando, C. R., Wang See, C., Chang, T.-Y., & Barabino, G. A. (2018). Changes in phenotype and differentiation potential of human mesenchymal stem cells aging in vitro. *Stem Cell Research & Therapy*, *9*(1), 131. https://doi.org/10.1186/s13287-018-0876-3

21. Chen AK-L, Chew YK, Tan HY, Reuveny S, Weng Oh SK. Increasing efficiency of human mesenchymal stromal cell culture by optimization of microcarrier concentration and design of medium feed. *Cytotherapy*. 2015;17(2):163-173. doi:10.1016/j.jcyt.2014.08.011

22. Frith JE, Thomson B, Genever PG. Dynamic three-dimensional culture methods enhance mesenchymal stem cell properties and increase therapeutic potential. Tissue Eng Part C Methods. 2010 Aug;16(4):735-49. doi: 10.1089/ten.TEC.2009.0432. PMID: 19811095.

23. Maleki M, Ghanbarvand F, Reza Behvarz M, Ejtemaei M, Ghadirkhomi E. Comparison of mesenchymal stem cell markers in multiple human adult stem cells. *Int J Stem Cells*. 2014;7(2):118-126. doi:10.15283/ijsc.2014.7.2.118

24. Zhu, C. H., Mouly, V., Cooper, R. N., Mamchaoui, K., Bigot, A., Shay, J. W., Di Santo, J. P., Butler-Browne, G. S., & Wright, W. E. (2007). Cellular senescence in human myoblasts is overcome by human telomerase reverse transcriptase and cyclin-dependent kinase 4: consequences in aging muscle and therapeutic strategies for muscular dystrophies. *Aging cell*, *6*(4), 515–523. https://doi.org/10.1111/j.1474-9726.2007.00306.x

25. Egger D, Tripisciano C, Weber V, Dominici M, Kasper C. Dynamic Cultivation of Mesenchymal Stem Cell Aggregates. *Bioengineering (Basel)*. 2018;5(2). doi:10.3390/bioengineering5020048

26. Bhang, S. H., Cho, S. W., La, W. G., Lee, T. J., Yang, H. S., Sun, A. Y., Baek, S. H., Rhie, J. W., & Kim, B. S. (2011). Angiogenesis in ischemic tissue produced by spheroid grafting of human adipose-derived stromal cells. *Biomaterials*, *32*(11), 2734–2747. https://doi.org/10.1016/j.biomaterials.2010.12.035

27. Ward, T. H., Cummings, J., Dean, E., Greystoke, A., Hou, J. M., Backen, A., Ranson, M., & Dive, C. (2008). Biomarkers of apoptosis. *British Journal of Cancer*, *99*(6), 841–846. https://doi.org/10.1038/sj.bjc.6604519

28. Kepp O, Senovilla L, Vitale I, Vacchelli E, Adjemian S, Agostinis P, Apetoh L, Aranda F, Barnaba V, Bloy N, Bracci L, Breckpot K, Brough D, Buqué A, Castro MG, Cirone M, Colombo MI, Cremer I, Demaria S, Dini L, Eliopoulos AG, Faggioni A, Formenti SC, Fučíková J, Gabriele L, Gaipl US, Galon J, Garg A, Ghiringhelli F, Giese NA, Guo ZS, Hemminki A, Herrmann M, Hodge JW, Holdenrieder S, Honeychurch J, Hu HM, Huang X, Illidge TM, Kono K, Korbelik

M, Krysko DV, Loi S, Lowenstein PR, Lugli E, Ma Y, Madeo F, Manfredi AA, Martins I, Mavilio D, Menger L, Merendino N, Michaud M, Mignot G, Mossman KL, Multhoff G, Oehler R, Palombo F, Panaretakis T, Pol J, Proietti E, Ricci JE, Riganti C, Rovere-Querini P, Rubartelli A, Sistigu A, Smyth MJ, Sonnemann J, Spisek R, Stagg J, Sukkurwala AQ, Tartour E, Thorburn A, Thorne SH, Vandenabeele P, Velotti F, Workenhe ST, Yang H, Zong WX, Zitvogel L, Kroemer G, Galluzzi L. Consensus guidelines for the detection of immunogenic cell death. Oncoimmunology. 2014 Dec 13;3(9):e955691. doi: 10.4161/21624011.2014.955691.

29. Steinberg ML, Defendi V. Transformation and Immortalization of Human Keratinocytes by SV40. *Journal of Investigative Dermatology*. 1983;81(1, Supplement):S131-S133. doi:10.1111/1523-1747.ep12540905

30. Ng PK, Li J, Jeong KJ, Shao S, Chen H, Tsang YH, Sengupta S, Wang Z, Bhavana VH, Tran R, Soewito S, Minussi DC, Moreno D, Kong K, Dogruluk T, Lu H, Gao J, Tokheim C, Zhou DC, Johnson AM, Zeng J, Ip CKM, Ju Z, Wester M, Yu S, Li Y, Vellano CP, Schultz N, Karchin R, Ding L, Lu Y, Cheung LWT, Chen K, Shaw KR, Meric-Bernstam F, Scott KL, Yi S, Sahni N, Liang H, Mills GB. Systematic Functional Annotation of Somatic Mutations in Cancer. Cancer Cell. 2018 Mar 12;33(3):450-462.e10. doi: 10.1016/j.ccell.2018.01.021. 10.1016/j.ccell.2018.01.021